GMR
The Original

SYNTHESIS, CHARACTERISATION, ANTIMICROBIAL ACTIVITY AND MOLECULAR DOCKING STUDIES OF NOVEL NICKEL(II) AND COBALT(II) COMPLEXES DERIVED FROM 4-AMINOANTIPYRINE DERIVATIVES

Kaushik Mestry[1], Dattatray Patil[2], Chetan Meher[3], Shoyeab Khan[4], Dattatraya Yedage[5], Vidyesh Jadhav[6], Kirti Mhatre Patil[7]

[1,2,3,4,5] Department of Chemistry, Kirti M. Doongursee College, Dadar (W) Mumbai-400028, India
[5]Department of Chemistry, DES's Willingdon College, Sangli- 416415, India
[6]The New College, Kolhapur, Maharashtra, India
[7]Bhaskar Waman Thakur College of Science, Yashwant Keshav Patil College of Commerce, Vidya Dayanand Patil College of Arts, Virar, India.
Email ID: mestrykaushik32@gmail.com[1], dvspatil@gmail.com[2], cmeher478@gmail.com[3], khanshoyeab@gmail.com[4], dbyedagedb@gmail.com[5]

ABSTRACT

The Ni(II) and Co(II) complexes derived from 4-aminoantipyrine derivatives were synthesized and characterised by IR, Mass, ^{1}H NMR, electronic spectra, magnetic moment, molar conductance, thermal analysis. The obtained analytical data shows the Novel Ni(II) and Co (II) complexes shows metal to ligand ratio 1:2. The ligand acts as bidentate ligand co-ordinated to central metal ion through azomethine nitrogen. The geometry of synthesized novel Ni(II) and Co(II) complexes were octahedral. The novel complexes were screened for their biological potential against selected strains of antibacterial and antifungal organism by broth dilution method. The molecular docking studies of Novel complexes against E. coli DNA Gyrase B (PDB ID: 6YD9) and Candida albicans lanosterol 14-α-demethylase (PDB ID: 5TZ1). The docking results demonstrate that the synthesized cobalt and nickel complexes exhibit consistently stronger affinity toward lanosterol 14-α-demethylase than toward DNA gyrase B, suggesting greater potential for antifungal activity.

KEYWORD: Ni(II) and Co(II) Complexes, Antimicrobial activity, 4-Aminoantipyrine, Molecular docking

GRAPHICAL ABSTRACT

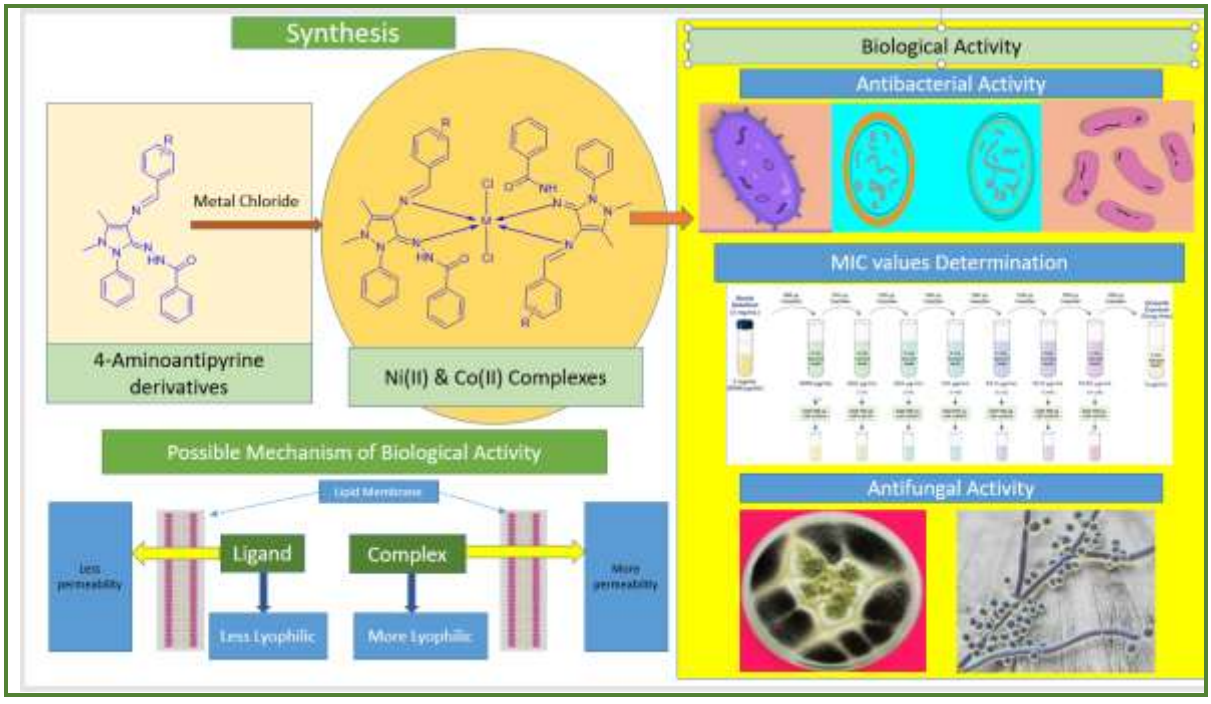

1.0 INTRODUCTION

Now a days there is increasing microbial resistance to various available antibiotics[1] hence there is need to search for novel derivatives with biological potential against pathogenic bacteria and fungi. The most impressive advances in the field of medicinal chemistry have been made by novel heterocyclic compounds with good biological potential [2]. It is observed that heterocyclic compounds are widely distributed in nature and some of these heterocycles are of interest due to many reasons, among which their biological potential towards variety of

species[3]. Many of the heterocycles act as drug with sulfur, oxygen, nitrogen, azomethine nitrogen and alcoholic or phenolic oxygen as donor atoms. Heterocyclic Compounds exhibit variety of physiological properties viz. analgesic [4], antioxidant [5–7], anti-inflammatory[8] and anti-cancer activity[9]. N-heterocyclic compound, serves as an active moiety in pharmaceutical formulations, particularly in nonsteroidal anti-inflammatory drugs (NSAIDs) used to treat conditions such as arthritis and various musculoskeletal and joint disorders.

Heterocycles like 4-aminoantipyrine is one of the Pyrazolone compound converted into variety of flexible heterocycle derivatives by condensation with various aldehydes and ketones. They were reported as superior reagents in biological, pharmacological, clinical and analytical applications. 4-Aminoantipyrine (4-amino-1,5-dimethyl-2-phenylpyrazole-3-one, 4-AAP) features a pyrazolone moiety with a five-membered nitrogen ring and a free amino group, structurally similar to N-substituted amides. Chemistry of pyrazolone has also received attention due to its variety of biological potential including antibacterial [10–14], antifungal [15], anticancer activity[16]. Their ligational behaviour is due to the presence of sp^2 hybridised orbital of the nitrogen atom of the azomethine group. The denticity of the derivatives of 4-aminoantipyrine increases with the presence of one or more donor atoms close to the azomethine group[17]. These derivatives are active and stable under a variety of oxidative and reductive conditions. Derivatives derived from 4-aminoantipyrine with a pyrazolone skeleton and its complexes have a variety of applications in areas including biological, clinical, analytical, and pharmacological applications[18]. Azomethine group of derivatives derived from 4-aminoantipyrine has electron-rich N center and electron-poor C center due to which various electrophile and nucleophile bind to it and thus derivatives show variety of biological applications [19].

First-row transition metals with biological significance, nickel and cobalt are vital to many biochemical processes. In a number of enzymes, such as urease, [NiFe]-hydrogenases, carbon monoxide dehydrogenase and methyl-coenzyme M reductase, nickel serves as a crucial catalytic metal center that supports nitrogen metabolism, hydrogen oxidation, and carbon cycle. Because of nickel's biological significance, coordination compounds containing nickel have been thoroughly studied as medicinal and bioactive substances. Similarly, because it forms the core metal ion of vitamin B12 (cobalamin), which takes part in cellular metabolism, DNA synthesis and methyl transfer processes, cobalt is a vital element in biological systems. Cobalt complexes are appealing options in medical inorganic chemistry due to the metal's special redox characteristics and coordination versatility[20]. Because of their different coordination geometries, oxidation states, and capacity to bind with multifunctional ligands, nickel and cobalt complexes exhibit extraordinary structural variety. They can interact with biological targets like DNA, proteins, enzymes and cellular membranes. Because metal coordination can drastically alter the biological behaviour of organic ligands therefore metal complexes including nickel and cobalt have been thoroughly studied for their antibacterial, antioxidant, DNA-interacting and anticancer capabilities[21].Significant antibacterial[22–24] action against several bacterial strains has been demonstrated by Nickel(II) and Cobalt(II) complexes made from 4-aminoantipyrine Schiff bases. Chelation-induced increases in lipophilicity[25], which enable contact with intracellular targets and improve penetration through microbial membranes, have been linked to these complexes increased antimicrobial efficiency[26,27]. A number of cobalt and nickel complexes with ligands generated from 4-aminoantipyrine have shown exceptional antifungal efficacy against pathogenic fungal species in addition to their antibacterial qualities. Such action has been linked to oxidative stress production inside fungal cells, disruption of fungal metabolic pathways and inhibition of vital enzymes, suggesting their potential use as antifungal drugs[28–30]. Significant attention has also been drawn to metal complexes capacity to control oxidative processes. Antioxidant activity has been demonstrated by nickel and cobalt complexes of Schiff base ligands generated from 4-aminoantipyrine, especially through free-radical scavenging methods like DPPH and associated tests. These characteristics imply that they may be used to manage biological illnesses linked to oxidative stress [31] and some of these complexes also shows anticancer activity[32]. Antimicrobial resistance is a global issue. The present antimicrobial agents fail to treat many microbial infections. This is a serious issue because infection may kill or spread to others and increase medical cost. Due to this reason, the development of novel antimicrobial drugs against resistant microbes is essential.

The present study deals with the synthesis of novel Nickel and Cobalt complexes of 4-aminoantipyrine and their characterization by IR, NMR, Mass, Thermal methods, Conductance and UV-Visible Spectroscopy. The synthesized novel derivatives were also evaluated for its biological potential against selected microorganism including antibacterial and antifungal by in vitro study and MIC value which was evaluated by serial dilution method.

2.1 MATERIAL AND METHOD

The aromatic aldehydes including benzaldehyde and bromo substituted benzaldehyde, benzohydarzide, Nickel chloride hexahydrate, Cobalt chloride hexahydrate, dimethyl formamide, absolute ethanol, ethyl acetate were purchased from Sigma Aldrich. The FTIR spectra were recorded on ATR from Bruker, NMR spectra were recorded on Bruker spectrometer at 600MHz with DMSO-d_6 as solvents and chemical shift were recorded in ppm. We recorded mass spectra on Waters mass spectrometer 3100 mass detector, electronic spectra were obtained by Perkin Elmer Lambda 365 instrument and thermal analysis were done on Thermogravimetric analyzer TGA 4000(Perkin Elmer), antibacterial, antifungal study were done at Biocyte, research and development Pvt. Ltd, Sangli. The magnetic susceptibility were recorded on Gouy balance. The molar conductance were recorded on Digital Auto ranging Conductivity meter made by equiptronics with model No. EQ 664A.Capillary method was used to determine the melting point of synthesized derivatives and metal complexes. Auto Dock Vina was

used in the molecular docking study to explore the binding affinity and interaction pattern of the synthesized cobalt (II) and nickel (II) complexes with the target proteins which are related to the antibacterial and antifungal drug properties. The crystal structures of *Escherichia coli* DNA gyrase B (PDB ID: 6YD9) and Candida albicans lanosterol 14-α-demethylase (CYP51) (PDB ID: 5TZ1) were downloaded from the PDB. All crystallographic water molecules, co-crystallized derivative and other non-essential heteroatoms were removed from the protein structures before docking. The missing H atoms were added, Kollman charges were added to the atoms, and the prepared proteins were stored in the PDBQT file format using Auto Dock Tools. The metal complexes were synthesized and their structures drawn with the help of Chem Draw software and then converted to PDB format. After that, the structures of these metal complexes were drawn using AutoDock Tools with the partial charges assigned using the Gasteiger method, rotatable bonds were assigned to suitable groups and the structures obtained were saved in the PDBQT format. The three-dimensional size of the grid box was determined by the dimension(s) of the binding cavity of each target protein, centered on the active site, based on the position of the co-crystallized derivative, to ensure complete coverage of the binding cavity and freedom of derivative movement during docking. For every metal complexes, several binding poses were generated and the binding pose with the lowest binding free energy (kcal/mol) and the most favourable interactions within the active site was chosen and analysed.

2.2 Synthesis of Novel Ni(II) and Cobalt(II) complexes

In continuous of our previous work, Novel Nickel(II) and Co(II) complexes were synthesized from 4-aminoantipyrine derivatives BDMPPBH, 2BrBDMPPVH, 3BrBDMPPBH, 4BrBDMPPBH (L1 –L4) prepared by reported method [33] .

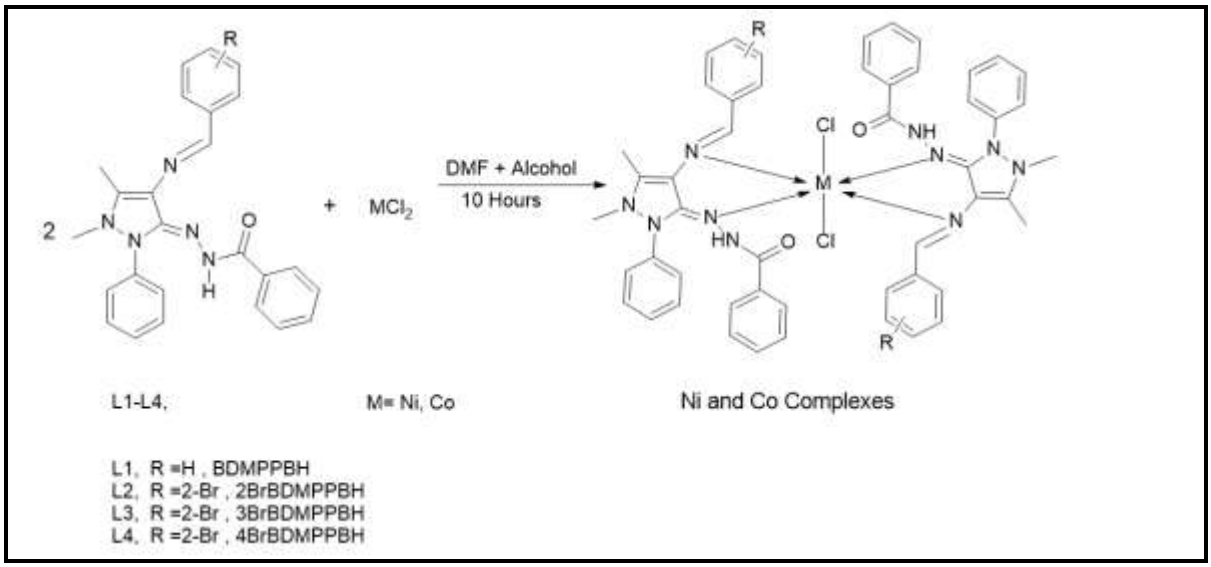

Scheme 1: Synthesis of Ni(II) and Co(II) Complexes

The novel Ni(II) and Co(II) complexes were prepared as shown in **Scheme 1** in which 1mmol of corresponding metal salt dissolve in minimum quantity of absolute ethanol and 2 mmol of corresponding 4-aminoantipyrine derivative BDMPPBH, 2BrBDMPPBH, 3BrBDMPPBH, 4BrBDMPPBH (L1-L4) in minimum quantity of dimethylformamide. The drop by drop corresponding metal salts were charged to derivatives (L1 –L4) and the resulting solution were refluxed at 150 **ºC** for about 10 hours. After completion of reaction the volume of reaction mixture was reduced to 1/3 of its volume then poured on crush ice and stirred to obtained corresponding metal complexes of Nickel and cobalt. The progress of reaction was monitored by using hexane: ethyl acetate system 8:2.

3.0 RESULT AND DISCUSSION

The 4-aminoantipyrine derivatives BDMPPBH, 2BrBDMPPBH, 3BrBDMPPBH, 4BrBDMPPBH (L1-L4) were white in colour as reported by our previous method[33]. The synthesised derivatives (L1-L4) and their corresponding novel metal complexes of Nickel (II) and Cobalt(II) were highly soluble in DMSO and DMF and very low solubility in alcohol and chloroform. There molecular weight, molecular formula, colour, melting point of 4-aminoantipyrine and their corresponding Ni(II) and Co(II) complexes were depicted in **Table 1 and 2** respectively. The mass spectrum of were depicted in supporting information in **Figure 1-12.**

Table 1: Physical Properties of 4-aminoantipyrine derivatives and their Ni(II) and Co(II) complexes

Entry	Derivative	Molecular Formula	Molecular weight Observed (Expected)	Colour	M.P (ºC)
1	BDMPPBH	$C_{25}H_{23}N_5O$	408.3(409.48)	White	207[33]

2	2BrBDMPPBH	$C_{25}H_{23}BrN_5O$	489.5(488.38)	White	210[33]
3	3BrBDMPPBH	$C_{25}H_{23}BrN_5O$	489.5(488.38)	White	170[33]
4	4BrBDMPPBH	$C_{25}H_{23}BrN_5O$	487.5(488.38)	White	179[33]

Table 2: Physical Properties of Ni(II) and Co(II) complexes derived from 4-aminoantipyrine derivatives

Entry	Complexes	Molecular Formula	Molecular weight Observed (Expected)	Colour	M.P (ºC)
1	Ni(II)BDMPPBH	$C_{50}H_{46}Cl_2N_{10}NiO_2$	947.5(948.57)	Light Cream	194
2	Ni(II)2BrBDMPPBH	$C_{50}H_{44}Br_2Cl_2N_{10}NiO_2$	1105.2(1106.36)	Olive Green	205
3	Ni(II)3BrBDMPPBH	$C_{50}H_{44}Br_2Cl_2N_{10}NiO_2$	1105.54(1106.3)	Golden Yellow	222
4	Ni(II)4BrBDMPPBH	$C_{50}H_{44}Br_2Cl_2N_{10}NiO_2$	1105.3(1106.36)	Light Brown	242
5	Co(II)BDMPPBH	$C_{50}H_{46}Cl_2N_{10}CoO_2$	947.63(948.81)	Brown	275
6	Co(II)2BrBDMPPBH	$C_{50}H_{44}Br_2Cl_2N_{10}CoO_2$	1105.3(1106.60)	Creamy Brown	190
7	Co(II)3BrBDMPPBH	$C_{50}H_{44}Br_2Cl_2N_{10}CoO_2$	1107.5(1106.60)	Brown	162
8	Co(II)4BrBDMPPBH	$C_{50}H_{44}Br_2Cl_2N_{10}CoO_2$	1105.4(1106.60)	Yellow	260

3.1 IR spectra

The IR spectra of Novel Ni(II) and Co(II) complexes and their corresponding derivatives were depicted in **Table 3**. The N-H streching frequency of hydrazide ranges from 3178 to 3377 cm^{-1}. The azomethine streching frequency in Nickel and Cobalt complexes due to hydrazide moiety ranges from 1600 – 1615 cm^{-1}. The azomethine streching frequency in Nickel and Cobalt complexes due to benzelidene moiety ranges from 1537 – 1576 cm^{-1}. The azomethine starching frequency due hydrazide moiety of in all the **Nickel complexes** shows shift in frequency upto 17 cm^{-1} while that of azomethine frequency of benzelidene moiety shows shift upto 23 cm^{-1}. The azomethine starching frequency due hydrazide moiety of in all the **cobalt complexes** shows shift in frequency upto 17 cm^{-1} while that of azomethine frequency of benzelidene moiety shows shift upto 23 cm^{-1}. The M-N stretching frequency in all the novel complexes appear in the range of 509 to 518 cm^{-1}. From shift in the stretching frequency of azomethine nitrogen and M-N streching frequency its conform the azomethine nitrogen is involved in coordination with central metal ion in the complex. The IR spectrum of Ni(II) and Co(II) complexes were depicted in supporting information in **Figure 13-24**.

Table 3 : IR spectrum of Novel Metal complexes and there corresponding derivatives

Derivative	υ (N-H) cm^{-1}	υ (Ar-CH) cm^{-1}	υ (Ali-CH) cm^{-1}	υ hydrazide (C=O) cm^{-1}	υ (C=N) hydrazide cm^{-1}	υ (C=N) benzyliedene cm^{-1}	υ (Ar-C=C) cm^{-1}	υ (M-N) cm^{-1}
BDMPPBH	3195.21	3058.04	2902.48	1639.67	1553.11	1599.02	1482.56	--
Ni(II)BDMPPBH	3178.48	3056.44	3028.18	1638.68	1576.30	1600.80	1486.95	510.94
Co(II)BDMPPBH	3178.09	3058.31	3027.97	1639.12	1552.11	1600.53	1486.78	510.44
2BrBDMPPBH	3187.44	3056.66	2902.31	1644.02	1556.94	1597.79	1467.05	--
Ni(II)2BrBDMPPBH	3180.97	3055.30	2849.91	1644.22	1557.80	1601.13	1493.10	512.22
Co(II)2BrBDMPPBH	3179.81	3052.78	2980.58	1671.30	1568.30	1615.91	1470.57	511.92
3BrBDMPPBH	3196.24	3057.35	2902.34	1646.75	1576.56	1599.85	1472.77	---
Ni(II)3BrBDMPPBH	3377.11	3217.29	3060.32	1640.85	1552.69	1605.97	1478.02	512.87
Co(II)3BrBDMPPBH	3377.16	3216.75	3065.64	1639.02	1553.96	1606.28	1478.74	512.42
4BrBDMPPBH	3273.04	3056.34	2901.51	1649.75	1537.00	1587.86	1470.65	---
Ni(II)4BrBDMPPBH	3273.98	3056.45	2918.69	1649.44	1537.33	1604.54	1479.85	510.21
Co(II)4BrBDMPPBH	3273.47	3056.32	3029.65	1649.54	1537.34	1604.40	1481.04	509.95

3.2 ^{1}H NMR spectra of complexes.

The azomethine proton in all Ni complexes derived from 4-aminoantipyine derivatives shows peak in the range of 8.42-8.82 while N-H proton shows peak in the range of 11.83-12.09.The azomethine peak of Co complexes appears in the range of 8.41-8.44 while N-H proton shows peak in the range of 11.85 to 12.12.The disappears of N-CH_3 and C-CH_3 peak in the complexes the bulky nature of aromatic hydrazides which lock the conformation and structure becomes rigid, planar so the molecule tumble slowly due to which the signal becomes weak or even broad which cannot be detected by NMR instrument [33]. The ^{1}H NMR data of complexes were depicted in **Table 4.** The ^{1}H NMR spectrum of Ni(II) and Co(II) complexes were depicted in supporting information in **Figure 25-32**.

Table 4: ^{1}H NMR of Ni(II) and Co(II) complexes

Complexes	N-H	H-C=N	Ar-H
Ni(II)BDMPPBH	11.83	8.45	7.91-7.43
Ni(II)2BrBDMPPBH	12.09	8.82	8.01-7.35
Ni(II)3BrBDMPPBH	11.97	8.41	7.90-7.41
Ni(II)4BrBDMPPBH	11.90	8.42	7.90-7.50
Co(II)BDMPPBH	11.85	8.48	7.93-7.47
Co(II)3BrBDMPPBH	12.12	8.84	8.04-7.38
Co(II)3BrBDMPPBH	11.97	8.41	7.92-7.40
Co(II)4BrBDMPPBH	11.92	8.84	7.93-7.53

3.3 Thermal analysis:

The thermal stability of metal complexes were studied by using TGA under Nitrogen atmosphere 20 ml per minute from 30 to 800 **ºC** and depicted in **Table 5**. The thermogram of all metal complexes shows no weight loss upto 200 **ºC** which indicated there is no co-ordinated water molecule in complexes [34]. The novel complexes were stable upto 300 **ºC.** The thermogram of Ni(II) and Co(II) complexes were depicted in supporting information in **Figure 33-40**

Table 5: Decomposition Temperature of metal complexes

Entry	Complexes	Decomposition temperature in ºC
1	Ni(II)DBMPPBH	304.19
2	Ni(II)2BrDBMPPBH	301.95
3	Ni(II)3BrDBMPPBH	334.33
4	Ni(II)4BrDBMPPBH	333.30
5	Co(II)DBMPPBH	314.96
6	Co(II)2BrDBMPPBH	300.69
7	Co(II)3BrDBMPPBH	317.40
8	Co(II)4BrDBMPPBH	337.74

3.4 Molar Conductivity:

Conductance of novel metal complexes derived from 4-aminoantipyrine derivatives (ligands) were measured on digital auto ranging conductivity meter with magnetic stirrer with cell constant 1.00 on Equiptronics Model No. EQ 664A. The molear conductance values were depicted in **Table 6**. The low value of molar conductivity reveals that they are non electrolyte in nature [35–37].

Table 6: Molar Conductance of Ni(II) and Co(II) complexes

Entry	Complexes	Specific conductance in μS 1000 ppm (k)	Molar concentration (C) $\times 10^{-3}$	Molar conductivity in S cm^2 mol^{-1} = 1000k / C
1	Ni(II)BDMPP	32.000	1.054	30.36

2	Ni(II)2BrBDMPP	1.387	0.903	1.535
3	Ni(II)3BrBDMPP	1.500	0.903	1.661
4	Ni(II)4BrBDMPP	2.100	0.903	2.325
5	Co(II)BDMPP	2.000	1.053	1.899
6	Co(II)2BrBDMPP	1.526	0.903	1.690
7	Co(II)3BrBDMPP	1.600	0.903	1.771
8	Co(II)4BrBDMPP	13.000	0.903	14.396

3.5 Magnetic susceptibility

Magnetic susceptibility data measured at room temperature (RT) by using Gouy's balance DHONA 100 with $Hg[Co(SCN)_4]$ as a standard. Effective magnetic moments of Novel Ni(II) and Co(II) were calculated after applying diamagnetic corrections for the ligand components using Pascal's constants.

The magnetic moments of Novel Ni(II) and Co(II) complexes of 4-aminoantipyrine derivatives were calculated by using following equations and depicted in Table

Mass of empty tube without magnetic field	=	W_1 g	---1
Mass of empty tube with applied magnetic field	=	W_2 g	---2
Difference in the mass of empty tube with and without magnetic field.	=	$\Delta x = W_2 - W_1$ g	---3
Mass of tube + standard without magnetic field	=	W_3 g	---4
Mass of tube + standard with the magnetic field	=	W_4 g	---5
Mass of standard	=	$W_s = W_3 - W_1$ g	---6
Mass difference of tube + standard with and without magnetic field	=	$\Delta y = W_4 - W_3$ g	---7
Final mass difference of standard	=	$\Delta W_s = \Delta y - \Delta x$ g	---8
Difference in mass of empty tube with and without magnetic field.	=	$\Delta m = W_2 - W_1$	---9
Mass of tube + complex without magnetic field	=	W_5 g	---10
Mass of tube + complex with magnetic field	=	W_6 g	---11
Mass difference of tube + complex with and without magnetic field.	=	$\Delta n = W_6 - W_5$ g	---12
Final difference in mass of complex	=	$\Delta Wc = \Delta n - \Delta m$	---13
Weight of complex	=	$W_c = w_5 - w_1$	---14
Magnetic susceptibility of complex in g $\chi_g = (\chi_g)_s \times (W_s / \Delta W_s) \times (\Delta W_c / W_c)$	=		---15
χ_g = gram susceptibility of the complex			
$(\chi_g)_s$ = gram susceptibility of the standard			
$\chi_M = \chi_g \times$ molecular weight = cgs units	=		---16
χ_M = molar susceptibility			
$\chi_M^{corr} = \chi_M$ – diamagnetic correction –TIP = cgs units	=		---16
TIP = temperature-independent paramagnetism			
$\mu_{eff} = 2.83(\chi_M T)^{1/2}$ = B.M.	=		---17

Table 7: Magnetic moment of Novel Complexes

Entry	Complex	χ_M^{corr}	μ_{eff}	Magnetism	High / Low Spin
1	Co(II)BDMPPBH	0.00861	4.534	Paramagnetic	High
2	Co(II)2BrBDMPPBH	0.00920	4.687	Paramagnetic	High
3	Co(II)3BrBDMPPBH	0.00899	4.632	Paramagnetic	High
4	Co(II)4BrBDMPPBH	0.00877	4.574	Paramagnetic	High
5	Ni(II)BDMPPBH	0.00395	3.074	Paramagnetic	High
6	Ni(II)2BrBDMPPBH	0.00384	3.029	Paramagnetic	High
7	Ni(II)3BrBDMPPBH	0.00391	3.058	Paramagnetic	High
8	Ni(II)4BrBDMPPBH	0.00369	2.968	Paramagnetic	High

The magnetic moment of all the novel complexes were depicted in Table On the basis of magnetic moment its conclude that all the Ni(II) and Co(II) complexes derived from novel 4-aminoantipyrine derivatives including BDMPPBH, 2BrBDMPPBH, 3BrBDMPPBH, 4BrBDMPPBH are paramagnetic in nature due to two and three unpaired electrons respectively and are high spin complexes.

4.0 Biological Applications:

The novel Nickel, Cobalt metal complexes derived from 4-aminoantipyrine derivatives were studied for their antibacterial potential against Escherichia coli, Staphylococcus aureus, Pseudomonas aeruginosa, Bacillus *subtilis* by broth dilution method. Culturing of microorganism, inoculum development and MIC determination were carried out in laminar air flow. Samples were prepared 2 mg/ml and then appropriately diluted at different serial dilutions ranging from 2mg to 0.25mg. The inoculum of cultures (single cultures) was developed in broth medium. The cultures were then incubated and subsequently, serially diluted to reach the density of 2×10^4 cells per ml. Cell counting was done using haemocytometer. Two millilitres of Nutrient broth/sabrouds dextrose broth was dispensed in tubes, and 100 µL of cell culture was inoculated in it. Then, 100 µL of different concentration of extract was added to each tube. Each experiment was carried out in a triplicate set. Growth control was run in parallel with every experiment. All the experimental tubes were incubated in incubator for 48 hours. After completion of incubation period, the optical density was measured at 600 nm using spectrophotometer. MIC was defined as the minimum concentration of extract that caused 20% inhibition in growth of test microorganism. The MIC values against tested microorganisms by BDMPPBH, 2BrBDMPPBH, 3BrBDMPPBH, 4BrBDMPPBH were used as reported by our previous study [33] as shown in **Figure 1** to compare the biological potential against the nickel and cobalt complexes. The antibacterial and antifungal activity data were depicted in supporting information From**Table 1-12.**

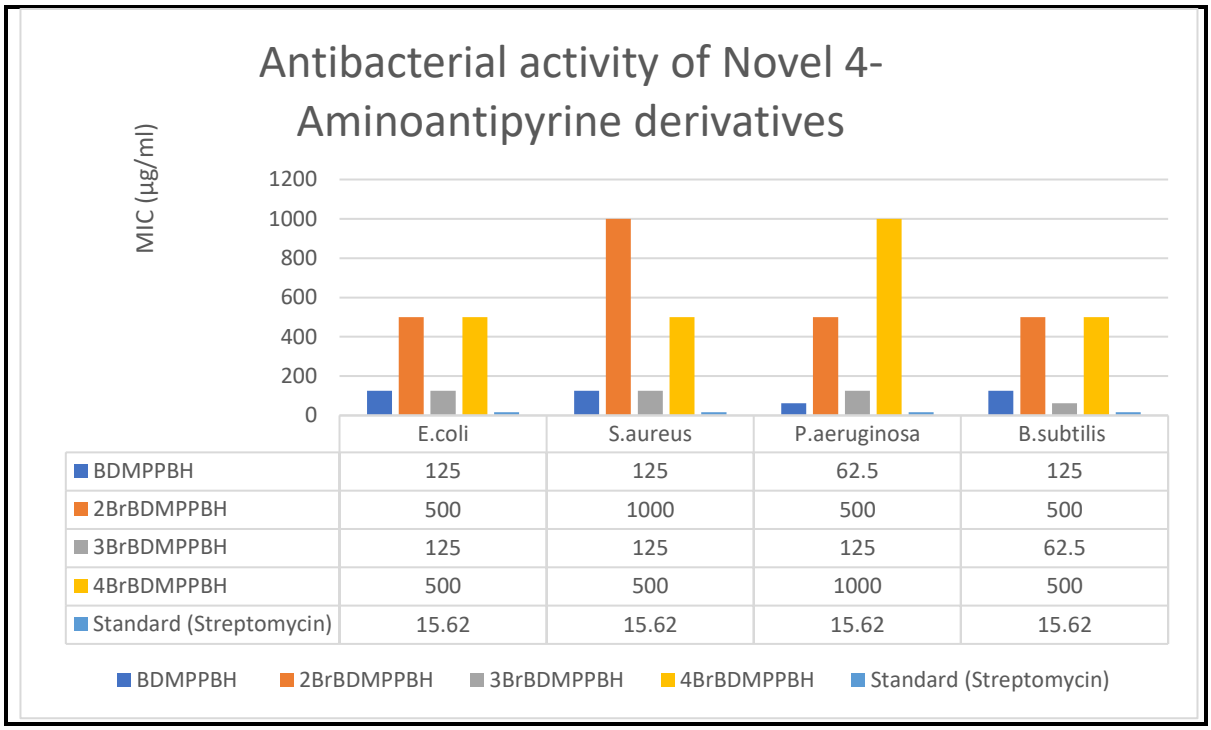

Figure 1: Antibacterial activity of Novel 4-Aminoantipyrine derivative

4.1 Antibacterial Activity of Nickel Complexes

The antibacterial potential of the synthesized Novel Ni(II) complexes of 4-aminoantipyrine derivatives demonstrated that metal coordination with novel ligands resulted in highly active antibacterial derivatives for both Gram-positive (*Staphylococcus aureus* and *Bacillus subtilis*) and Gram-negative (*Escherichia coli* and *Pseudomonas aeruginosa*) bacterial strains. The results revealed that the Ni(II) complexes exhibited excellent antibacterial efficacy, with MIC values ranging from **62.5 to 125 µg/mL**, indicating their potential as promising antibacterial agents. Among the synthesized novel Ni(II) complexes **Ni(II)BDMPPBH**, **Ni(II)2BrBDMPPBH** and **Ni(II)3BrBDMPPBH** emerged as the most potent antibacterial derivatives, each exhibiting a uniform MIC value of **62.5 µg/mL** against all four tested bacterial strains. The **Ni(II)4BrBDMPPBH** complex also displayed significant antibacterial activity, with MIC values of **62.5 µg/mL** against *Escherichia coli*, *Staphylococcus aureus* and *Bacillus subtilis*. However, a slightly higher MIC value (**125 µg/mL**) was observed against *Pseudomonas aeruginosa*, suggesting a comparatively lower inhibitory effect toward this microorganism. The MIC values of Ni(II) complexes against the bacterial strains were depicted in **Figure 2.**

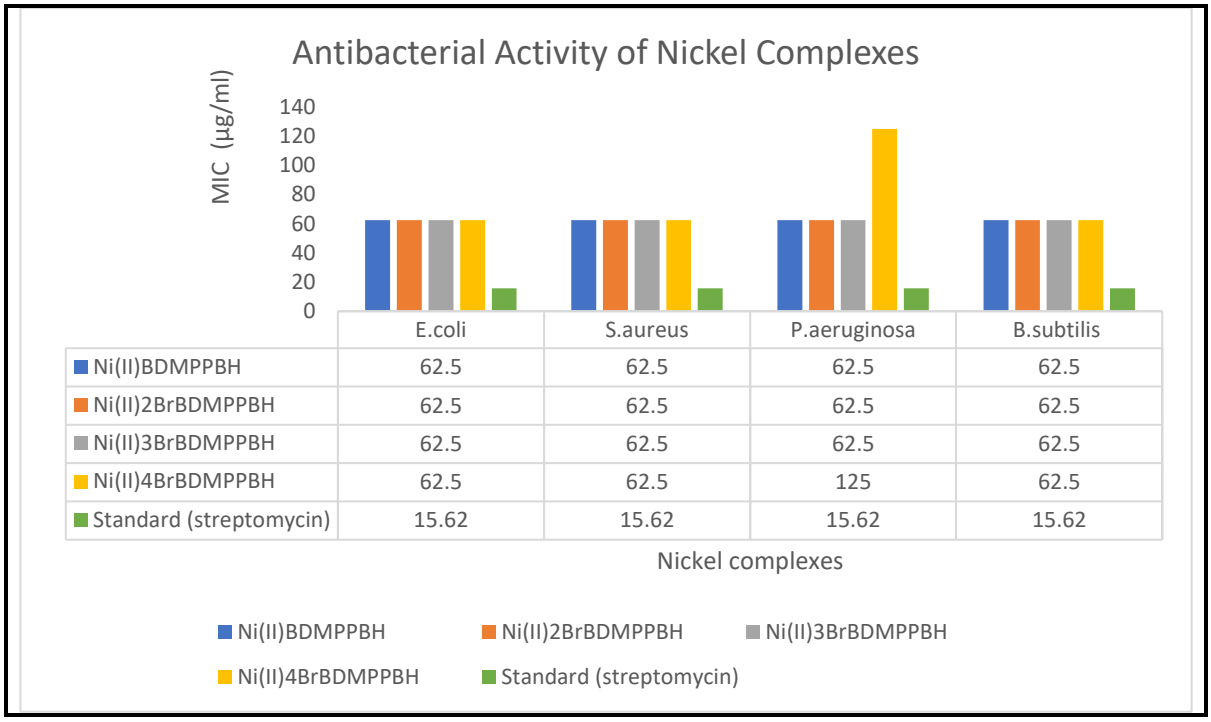

Figure 2: Antibacterial activity of Ni (II) complexes of 4-Aminoantipyrine derivative

Compared with their corresponding free derivatives, all Ni(II) complexes exhibited lower MIC values, confirming the positive influence of metal complexation on antibacterial efficacy. Among these complexes **Ni(II)2BrBDMPPBH** exhibited the greatest improvement over its parent derivative, with MIC values decreasing from **500–1000 µg/mL** to **62.5 µg/mL** against all tested bacterial strains. Similarly, **Ni(II)BDMPPBH** and **Ni(II)3BrBDMPPBH** showed enhanced antibacterial activity compared with their respective parent derivative, while **Ni(II)4BrBDMPPBH** also demonstrated a marked improvement despite showing slightly lower activity against *Pseudomonas aeruginosa*. Overall, the antibacterial activity of the synthesized Ni(II) complexes followed the order: **Ni(II)BDMPPBH ≈ Ni(II)2BrBDMPPBH ≈ Ni(II)3BrBDMPPBH > Ni(II)4BrBDMPPBH.**

4.2 Antibacterial Activity of Cobalt Complexes

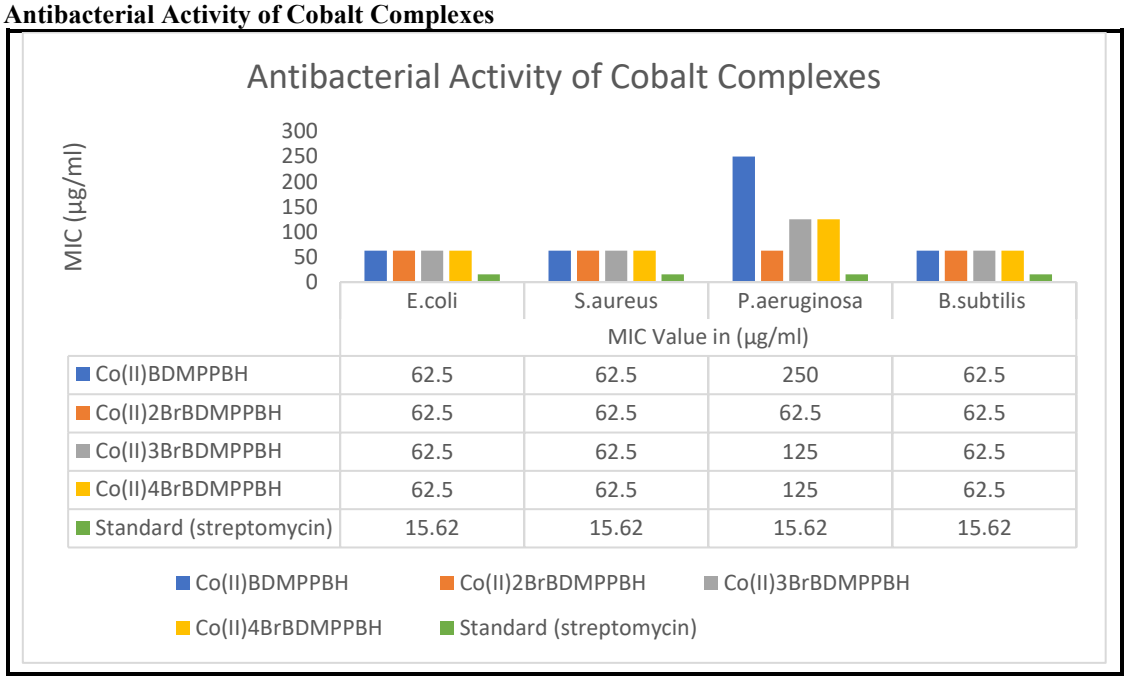

Figure 3: Antibacterial activity of Co (II) complexes of 4-Aminoantipyrine derivative

The antibacterial evaluation of the synthesized novel Co(II) complexes of 4-aminoantipyrine derivatives demonstrated that coordination with Co(II) significantly enhanced the antibacterial potential of the ligands against both Gram-positive (*Staphylococcus aureus* and *Bacillus subtilis*) and Gram-negative (*Escherichia coli* and *Pseudomonas aeruginosa*) bacterial strains. The synthesized Co(II) complexes exhibited excellent antibacterial efficacy, with MIC values ranging from **62.5 to 250 µg/mL**, highlighting their promising antimicrobial potential. Among the synthesized Co(II) complexes, **Co(II)2BrBDMPPBH** emerged as the most active antibacterial

derivative, exhibiting a uniform MIC value of **62.5 µg/mL** against all four tested bacterial strains, indicating excellent antibacterial activity. The **Co(II)3BrBDMPPBH** and **Co(II)4BrBDMPPBH** complexes also displayed appreciable antibacterial activity, with MIC values of **62.5 µg/mL** against *Escherichia coli*, *Staphylococcus aureus* and *Bacillus subtilis* and **125 µg/mL** against *Pseudomonas aeruginosa*. The **Co(II)BDMPPBH** complex exhibited significant antibacterial activity against *Escherichia coli*, *Staphylococcus aureus* and *Bacillus subtilis* (MIC = **62.5 µg/mL**), while showing a comparatively higher MIC value of **250 µg/mL** against *Pseudomonas aeruginosa.* Compared with their corresponding free derivatives, all the synthesized Co(II) complexes exhibited enhanced antibacterial activity as evidenced by the lower MIC values against the tested bacterial strains. **Co(II)BDMPPBH** showed improved activity against *Escherichia coli*, *Staphylococcus aureus*, and *Bacillus subtilis*, although it exhibited comparatively lower activity against *Pseudomonas aeruginosa*. **Co(II)2BrBDMPPBH** exhibited the most significant enhancement, with MIC values decreasing from **500–1000 µg/mL** for the derivative to **62.5 µg/mL** against all tested bacterial strains. **Co(II)3BrBDMPPBH** displayed improved antibacterial activity particularly against *Escherichia coli* and *Staphylococcus aureus*, while maintaining good activity against *Pseudomonas aeruginosa* and *Bacillus subtilis*. Similarly, **Co(II)4BrBDMPPBH** also demonstrated a good antibacterial potency compared with its parent derivative, with substantially lower MIC values against all the tested microorganisms. Overall, Co(II) coordination significantly enhanced the antibacterial efficacy of all the synthesized derivatives, with **Co(II)2BrBDMPPBH** emerging as the most promising antibacterial complex. Overall, the antibacterial activity of the synthesized Co(II) complexes followed the order: **Co(II)2BrBDMPPBH > Co(II)3BrBDMPPBH ≈ Co(II)4BrBDMPPBH > Co(II)BDMPPBH.** The MIC values of Co (II) complexes were depicted in **Figure 3.**

4.3 Antifungal Activity:

Using the broth dilution method, the MIC values of 4-aminoantipyrine derivatives and their Nickel, Cobalt, Zinc and Mercury metal complexes with corresponding derivatives on Candida albicans and Aspergillus niger was determined. Microorganism cultivation, inoculum creation and MIC measurement were done in following incubation, culture were serially diluted to density of 2×10^4 cells per millilitre. A hemocytometer was used for cell counts. 100 microliter of cell culture were injected into tubes filled with nutrient broth / sabrouds dextrose broth. Subsequently, each extract was put to each tube concentration was extracted. Every experiment was conducted in three sets. Every experiment was conducted concurrently with growth control. For 48 hours, every experimental tube was kept in an incubator. The measurement was completed at 600 nm. MIC was defined as the lowest extract concentration that inhibited the growth of the test microorganism by 20%.. The MIC values against tested microorganisms by BDMPPBH, 2BrBDMPPBH, 3BrBDMPPBH, 4BrBDMPPBH were used as reported by our previous study [33] as shown in **Figure 4** to compare the biological potential against the nickel and cobalt complexes.

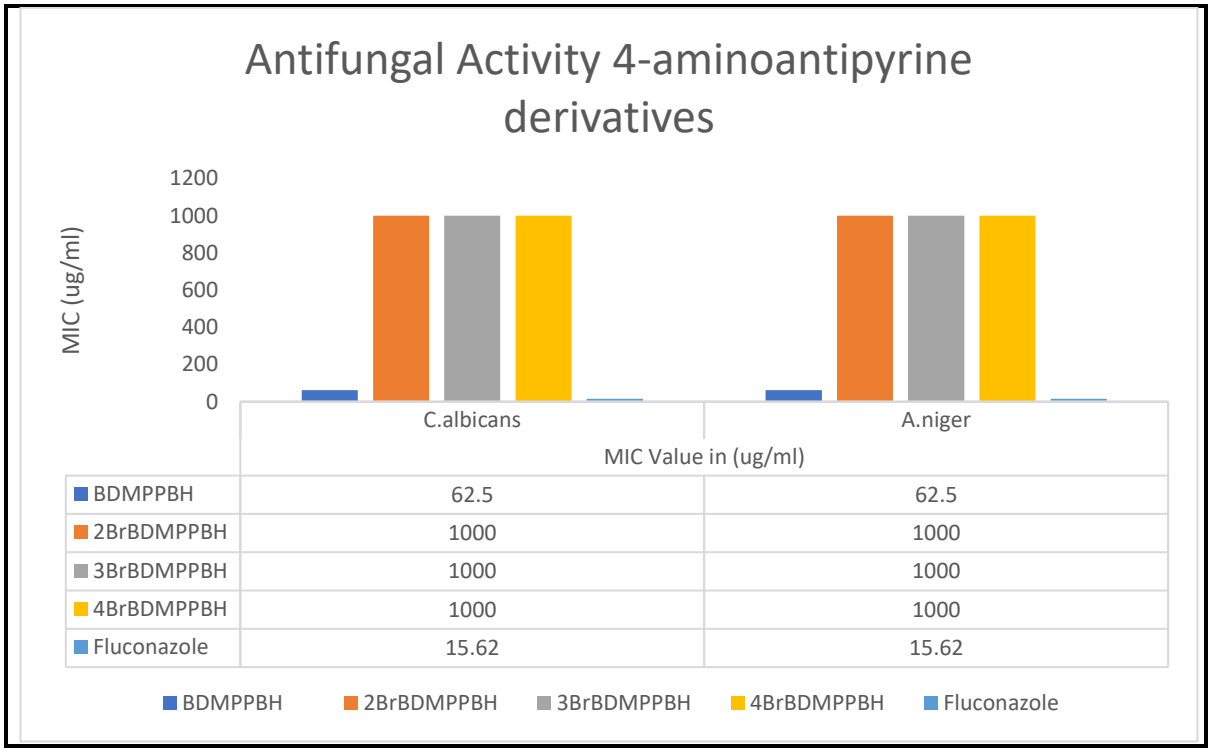

Figure 4: Antifungal activity of Novel 4-Aminoantipyrine derivative

4.4. Antifungal Activity of Nickel complexes

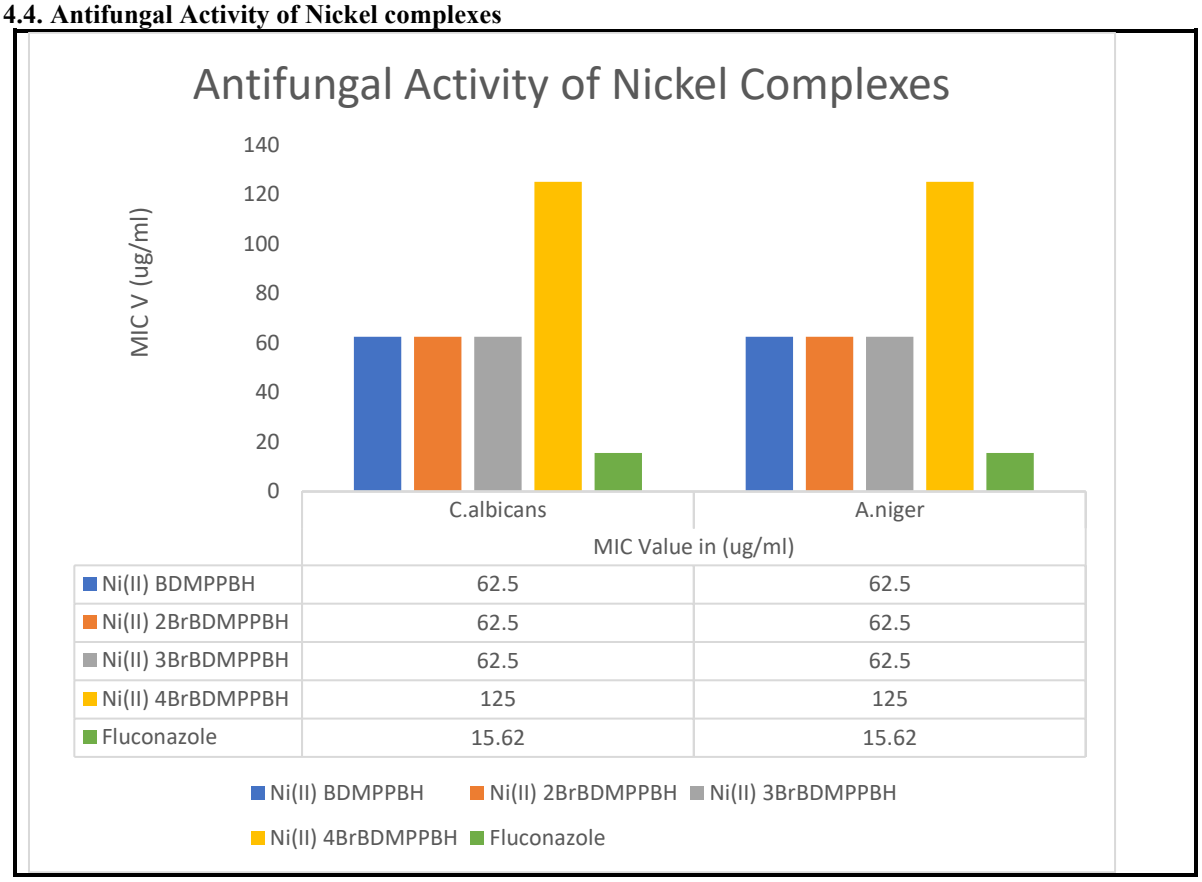

Figure 5: Antifungal activity of Ni (II) complexes of 4-Aminoantipyrine derivative

The antifungal evaluation of the novel Ni(II) complexes of 4-aminoantipyrine derivatives demonstrated that coordination with Ni(II) significantly enhanced the antifungal potential against both *Candida albicans* and *Aspergillus niger*. The synthesized Ni(II) complexes exhibited excellent antifungal efficacy, with MIC values ranging from **62.5 to 125 µg/mL**, highlighting their promising antifungal potential. Among, the novel synthesized Ni(II) complexes, **Ni(II)2BDMPPBH, Ni(II)3Br BDMPPBH and Ni(II)4BrBDMPPBH** emerged as the most potent antifungal derivatives, each having MIC values of **62.5-125 µg/mL** against both strains Candida albicans and Aspergillus niger, demonstrating antifungal activity. Overall, the antifungal activity of the produced Ni(II) complexes followed the order: **Ni(II)BDMPPBH ≈ Ni(II)2Br BDMPPBH ≈ Ni(II)3Br BDMPPBH > Ni(II)4Br BDMPPBH**. Comparison of the Ni(II) complexes with their corresponding parent derivatives revealed that the effect of metal coordination depended on the nature of the ligand. **Ni(II)BDMPPBH** exhibited antifungal activity identical to that of its parent derivative, with both showing MIC values of **62.5 µg/mL** against *Candida albicans* and *Aspergillus niger*, indicating that Ni(II) coordination neither enhanced nor diminished the antifungal. In contrast, **Ni(II)2BrBDMPPBH** and **Ni(II)3BrBDMPPBH** demonstrated a remarkable enhancement in antifungal activity, with MIC values decreasing from **1000 µg/mL** for the corresponding free ligands to **62.5 µg/mL** against both fungal strains after coordination with Ni(II). Similarly, **Ni(II)4BrBDMPPBH** also exhibited a significant improvement in antifungal potency, with MIC values decreasing from **1000 µg/mL** for the parent derivative to **125 µg/mL** against both *Candida albicans* and *Aspergillus niger*. Overall, Ni(II) coordination markedly enhanced the antifungal efficacy of the brominated derivatives, particularly **Ni(II)2BrBDMPPBH** , **Ni(II)3BrBDMPPBH** and **Ni(II)4BrBDMPPBH** while **Ni(II)BDMPPBH** maintained the antifungal activity of its corresponding parent derivatives. The MIC values of Ni(II) complexes against the fungal strains were depicted in **Figure 5.**

4.5 Antifungal Activity of Cobalt complexes

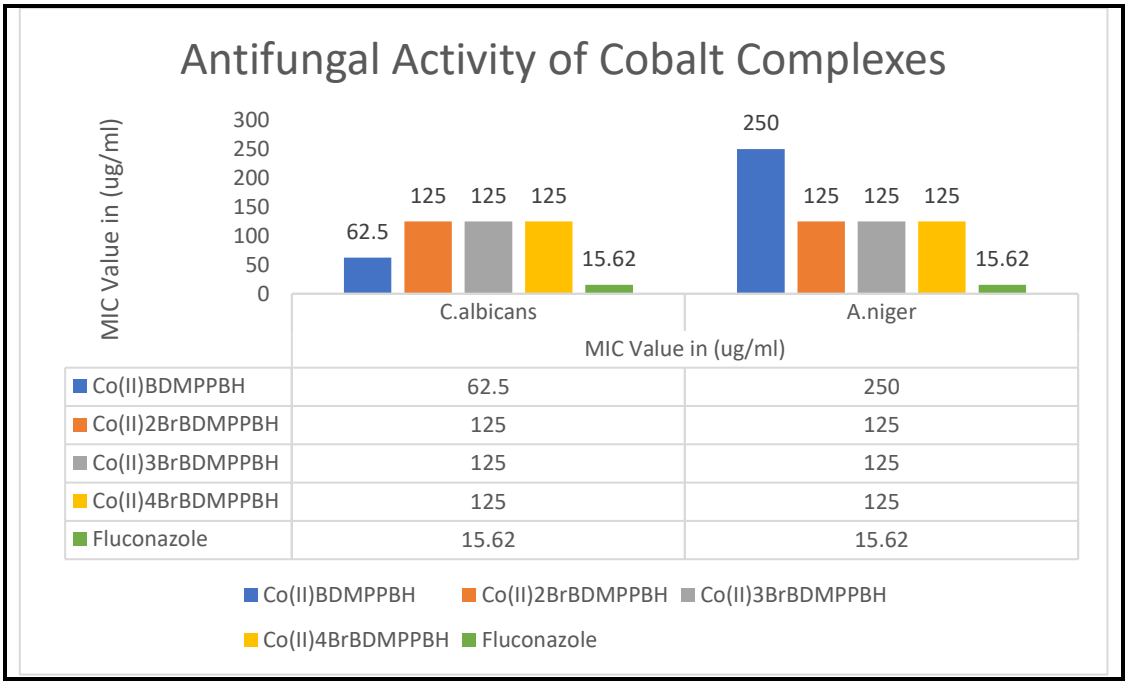

Figure 6: Antifungal activity of Co(II) complexes of 4-Aminoantipyrine derivative

The antifungal evaluation of the novel Co(II) complexes of 4-aminoantipyrine derivatives demonstrated that coordination with Co (II) significantly enhanced the antifungal potential against both *Candida albicans* and *Aspergillus niger*. The synthesized Co(II) complexes exhibited excellent antifungal efficacy, MIC values ranging from **62.5 to 250 µg/mL**, the synthesized Co(II) complexes demonstrated antifungal activity, suggesting their potential as antifungal agent. With a minimum inhibitory concentration (MIC) of **62.5 µg/mL**, **Co(II)BDMPPBH** was shown to be the most effective antifungal derivative against Candida albicans among the synthesized Co(II) complexes. With equivalent MIC values of **125 µg/mL** against Aspergillus niger and Candida albicans, the **Co(II)2BrBDMPPBH, Co(II)3Br BDMPPBH and Co(II)4Br BDMPPBH** complexes demonstrated similar antifungal efficacy. Overall, the synthesized Co(II) complexes antifungal activity was in the following order: **Co(II)2BrBDMPPBH ≈ Co(II)3BrBDMPPBH ≈ Co(II)4BrBDMPPBH > Co(II)BDMPPBH.** The synthesized Co(II) complexes showed varying antifungal efficacy against Aspergillus niger and Candida albicans when compared to their equivalent parent derivative. **Co(II)BDMPPBH** showed diminished activity against Aspergillus niger (MIC = 250 µg/mL) but maintained the antifungal activity of its parent derivative against Candida albicans (MIC = 62.5 µg/mL). **Co(II)2BrBDMPPBH, Co(II)3BrBDMPPBH and Co(II)4BrBDMPPBH** on the other hand, demonstrated a significant increase in antifungal activity; MIC values against both fungal strains dropped from **1000 µg/mL** for the respective parent derivatives to **125 µg/mL**. The MIC values of Co(II) complexes against the fungal strains were depicted in **Figure 6.**

5.0 MOLECULAR DOCKING STUDY

5.1 Molecular docking analysis Novel Ni (II) and Co(II) complexes against E. coli DNA Gyrase B (PDB ID: 6YD9)

The synthesized nickel cobalt and complexes of novel 4-aminaoantipyrine derivatives exhibited favourable binding affinities toward E. coli DNA gyrase B (PDB ID: 6YD9), with docking scores ranging from -6.7 to -8.2 kcal/ mol and represented in **Table 8** suggesting their potential as antibacterial agents through inhibition of the ATPase domain of DNA gyrase. Among the novel nickel complexes, **Ni(II)2BrBDMPPBH** demonstrated the strongest binding affinity of the entire series with a docking score of -8.2 kcal/mol. The complex formed an extensive interaction network consisting of π-π T-shaped interaction with His99, π-alkyl interactions with Ile78, Ile94, and Ala53, an alkyl interaction with Pro79, and a conventional hydrogen bond with Arg76. These interactions collectively indicate excellent accommodation within the ATP-binding site and explain its superior docking score. **Ni(II)BDMPPBH** exhibited a docking score of -7.8 kcal/mol, stabilized primarily through a π-cation interaction with His38 and a π-sigma interaction involving Thr34. Although the number of interactions was limited, their location within the active site likely contributes to stable binding. **Ni(II)4BrBDMPPBH** showed a docking score of -7.4 kcal/mol, establishing hydrophobic interactions with Ala53, Leu52, Pro79, Ile78, and Ile94, in addition to a conventional hydrogen bond with Arg76. This combination of hydrophobic and hydrogen-bond interactions supports moderate binding affinity. In contrast, **Ni(II)3BrBDMPPBH** displayed the lowest affinity (-6.7 kcal/mol), despite interacting with Arg76, Pro79, Ile94, and His99. The reduced docking score suggests that the orientation of the complex within the binding cavity may be less favourable, resulting in weaker overall binding. Among the cobalt complexes of novel 4-aminoantipyrine derivatives, **Co(II)2BrBDMPPBH** displayed the highest binding affinity with a docking score of -7.8 kcal/mol. This complex established multiple hydrophobic interactions with Pro79, Ile78, and Ala53, together with a π-cation interaction involving His99 and

a π-sigma interaction with Ile94. These residues are located within the ATP-binding pocket of GyrB and contribute significant stabilization. The combination of hydrophobic contacts and electrostatic interactions indicates a stable binding orientation within the catalytic cavity. **Co(II)BDMPPBH** demonstrated a docking score of -7.4 kcal/mol, forming π-π T-shaped interaction with His38 along with π-alkyl interactions involving Lys189 and Ile186. Although fewer interactions were observed compared to **Co(II)2BrBDMPPBH**, the aromatic interaction with His38 may contribute to stabilization of the complex within the binding pocket. Similarly, **Co(II)3BrBDMPPBH** exhibited a docking score of -7.3 kcal/mol, interacting with several catalytically important residues including Arg76, Asp49, Glu50, Ala53, His99, Val93, and Ile94. The simultaneous presence of π-cation (Arg76 and Asp49), π-anion (Glu50), π-π T-shaped (His99), and hydrophobic interactions suggests a well-balanced interaction network capable of enhancing binding stability. **Co(II)4BrBDMPPBH** showed a comparable docking score (-7.2 kcal/mol) and formed π-cation interaction with His99, a conventional hydrogen bond with Ile94, and hydrophobic interaction with Ile78. The presence of hydrogen bonding may partially compensate for its relatively fewer hydrophobic contacts. Overall, several residues including His99, Arg76, Ile78, Ile94, Ala53, and Pro79 repeatedly participated in ligand binding across both cobalt and nickel complexes, indicating that these amino acids constitute the principal interaction hotspot of the GyrB ATP-binding pocket. The superior performance of **Ni(II)2BrBDMPPBH**, followed by **Co(II)2BrBDMPPBH** and **Ni(II)BDMPPBH**, suggests that the metal center influences ligand orientation and interaction geometry, with the nickel complex exhibiting slightly enhanced affinity toward DNA gyrase B. Different interaction of Ni(II) and Co(II) complexes with **E. coli DNA Gyrase B (PDB ID: 6YD9)** in 3D were depicted in **Figure 7.**

Table 8: Molecular docking scores (kcal/mol) and protein-ligand interaction profiles of synthesized cobalt (II) and nickel (II) complexes against Escherichia coli DNA gyrase B (PDB ID: 6YD9)

Entry	Complexes	Docking score kcal / mol	
		E. coli **DNA Gyrase B (PDB ID: 6YD9)**	**Interacting Residues**
1	Ni(II)BDMPPBH	-7.8	His38, Pi-Cation; Thr34, Pi-Sigma;
2	Ni(II)2BrBDMPPBH	-8.2	His99, Pi-Pi T-Shaped; Ile94, Pi-Alkyl; Ile78, Pi-Alkyl; Ala53, Pi-Alkyl; Arg76, Conventional Hydrogen Bond; Pro79, Alkyl
3	Ni(II)3BrBDMPPBH	-6.7	Arg76, Pi-Cation; Ile94, Pi-Alkyl; His99, Pi-Pi T-shaped; Pro79, Carbon Hydrogen bond, Pi-Alkyl
4	Ni(II)4BrBDMPPBH	-7.4	Ala53, Pi-Alkyl; Leu52, Pi-Alkyl; Pro79, Alkyl; Arg76, Conventional Hydrogen Bond; Ile94, Pi-Alkyl; Ile78, Alkyl
5	Co(II)BDMPPBH	-7.4	His38, Pi-Pi T-Shaped; Lys189, Pi-Alkyl; Ile186, Pi-Alkyl
6	Co(II)2BrBDMPPBH	-7.8	Pro79, Pi-Alkyl; Ile78, Pi-Alkyl; Ala53, Pi-Alkyl; His99, Pi-Cation; Ile94, Pi-Sigma
7	Co(II)3BrBDMPPBH	-7.3	Arg76, Pi-Cation; Asp49, Pi-Cation; Glu50, Pi-Anion; Ala53, Pi-Alkyl; His99, PI-Pi T-Shaped; Val93, Alkyl; Ile94, Pi-Alkyl
8	Co(II)4BrBDMPPBH	-7.2	Ile78, Alkyl; His99, Pi-Cation;

			Ile94, Conventional Hydrogen Bond

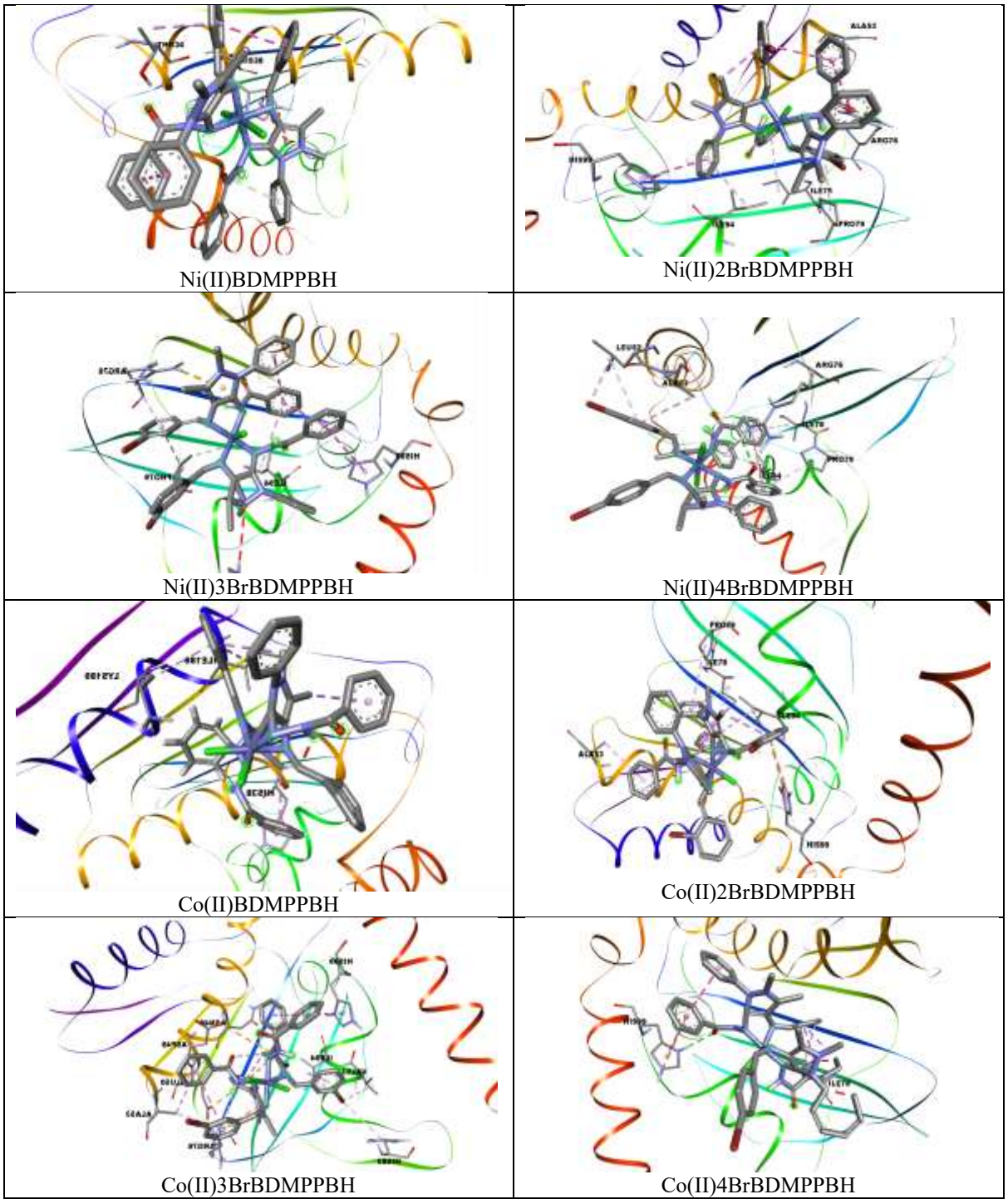

Figure 7: 3D Molecular docking study of Ni(II) and Co(II) complexes against Escherichia coli DNA gyrase B

5.2 Molecular docking analysis of Novel Ni (II) and Co(II) against Candida albicans lanosterol 14-α-demethylase (PDB ID: 5TZ1)

Docking studies against Candida albicans lanosterol 14-α-demethylase (CYP51; PDB ID: 5TZ1) revealed stronger binding affinities than those observed for DNA gyrase B, with docking scores ranging from -7.2 to -9.2 kcal/mol and are represented in **Table 9.** These findings indicate that the synthesized metal complexes possess promising antifungal potential by targeting the ergosterol biosynthesis pathway. **Ni(II)BDMPPBH** demonstrated a docking score of -8.1 kcal/mol, interacting primarily through hydrophobic contacts with Pro462, Lys367, and Leu461. Although no conventional hydrogen bonds were observed, the favourable hydrophobic environment contributed to stable complex formation. **Ni(II)3BrBDMPPBH** showed a docking score of -7.9 kcal/mol, exhibiting π-cation interaction with Lys367, π-anion interactions involving Arg469 and Glu473, π-π interaction with Tyr460, and hydrophobic interactions with Lys433 and Pro462. These interactions indicate stable accommodation within the active pocket despite its slightly reduced affinity compared with **Ni(II)4BrBDMPPBH**. **Ni(II)2BrBDMPPBH**

exhibited the lowest binding affinity among the nickel complexes (-7.5 kcal/mol), forming π-cation interaction with Glu444, π-anion interaction with Arg469, hydrogen bond with Ser453, π-alkyl interaction with Leu461 and a carbon hydrogen bond with Tyr460. Although several interactions were present, their spatial arrangement may not have provided optimal stabilization of the ligand. Among the novel cobalt complexes of 4-aminoantipyrinederivative, **Co(II)3BrBDMPPBH** exhibited the strongest binding affinity with a docking score of -9.2 kcal/mol. The complex formed π-alkyl interaction with Lys433, π-cation interaction with Arg469, π-anion interaction with Glu473, and a carbon hydrogen bond with Ser436. The simultaneous presence of electrostatic and hydrophobic interactions provides substantial stabilization of the ligand within the enzyme active site and likely accounts for its superior binding affinity. **Co(II)2BrBDMPPBH** closely followed with a docking score of -8.8 kcal/mol. This complex established multiple hydrophobic interactions involving Lys433, Val437, and Pro462, together with π-cation interaction with Arg469, π-anion interaction with Glu473, and π-π T-shaped interaction with Tyr460. The extensive interaction network indicates efficient occupation of the binding cavity and strong ligand stabilization. **Co(II)4BrBDMPPBH** demonstrated a docking score of -8.2 kcal/mol, forming conventional hydrogen bonds with Arg469 and Glu444, a halogen bond with Ile471, and a π-anion interaction with Glu473. The presence of multiple hydrogen-bonding interactions likely contributes significantly to its binding stability despite a slightly lower docking score. **Co(II)BDMPPBH** showed the lowest affinity among the cobalt complexes (-7.2 kcal/mol), interacting through hydrogen bonding with Arg142, π-cation interaction with Arg168, and hydrophobic interactions involving Val133 and Ile140. Although these interactions support stable binding, their distribution appears less optimal compared to the higher-scoring cobalt analogues. Interestingly, Arg469, Glu473, Lys433, Tyr460, Pro462, and Lys367 were repeatedly involved in ligand recognition across both cobalt and nickel complexes, suggesting that these residues play a central role in stabilizing inhibitor binding within the CYP51 active site. The strongest binding observed for **Co(II)3BrBDMPPBH** (-9.2 kcal/mol) and Ni_5d **Ni(II)4BrBDMPPBH** (-8.9 kcal/mol) indicates that coordination with different transition metals significantly influences the binding orientation and interaction profile of the Schiff base ligands. Different interaction ofNi(II) and Co(II) complexes with **Candida albicans lanosterol 14-α-demethylase (CYP51; PDB ID: 5TZ1) were depicted in Figure 8.**

Overall, the docking results demonstrate that the synthesized cobalt and nickel complexes exhibit consistently stronger affinity toward lanosterol 14-α-demethylase than toward DNA gyrase B, suggesting greater potential for antifungal activity.

Table 9: Molecular docking scores (kcal/mol) and protein-ligand interaction profiles of synthesized cobalt (II) and nickel (II) complexes against Candida albicans lanosterol 14-α-demethylase (CYP51; PDB ID: 5TZ1).

Entry	Complexes	Docking score kcal / mol	
		C. albicans lanosterol 14-alpha demethylase (PDB ID: 5TZ1)	Interacting Residues
1	Ni(II)BDMPPBH	-8.1	Pro462, Pi-Alkyl; Lys367, Pi-Alkyl; Leu461, Pi-Sigma
2	Ni(II)2BrBDMPPBH	-7.5	Glu444, Pi-Cation; Arg469, Pi-Anion; Ser453, Conventional Hydrogen bond; Leu461, Pi-Alkyl Tyr460, Carbon Hydrogen Bond
3	Ni(II)3BrBDMPPBH	-7.9	Arg469, Pi-Anion; Glu473, Pi-Anion; Lys367, Pi-Cation; Lys433, Pi-Alkyl; Tyr460, Pi-Pi T-shaped; Pro462, Pi-Alkyl
4	Ni(II)4BrBDMPPBH	-8.9	Lys367, Pi-Cation; Tyr460, Pi-Pi T-shaped; Glu473, Pi-Anion; Arg469, Pi-Cation; Lys433, Pi-Alkyl
5	Co(II)BDMPPBH	-7.2	Val133, Pi-Sigma; Ile140, Pi-Alkyl; Arg142, Conventional Hydrogen Bond; Arg168, Pi-Cation
	Co(II)2BrBDMPPBH	-8.8	Lys433, Pi-Alkyl; Val437, Pi-Alkyl;

6			Pro462, Pi-Alkyl; Arg469. Pi-Cation; Glu473, Pi-Anion; Tyr460, Pi-Pi T-shaped
7	Co(II)3BrBDMPPBH	-9.2	Lys433, Pi-Alkyl; Glu473, Pi-Anion; Arg469, Pi-Cation; Ser436, Carbon hydrogen bond
8	Co(II)4BrBDMPPBH	-8.2	Glu473, Pi-Anion; Arg469, Conventional Hydrogen Bond; Ile471, Halogen bond; Glu444, Conventional Hydrogen Bond

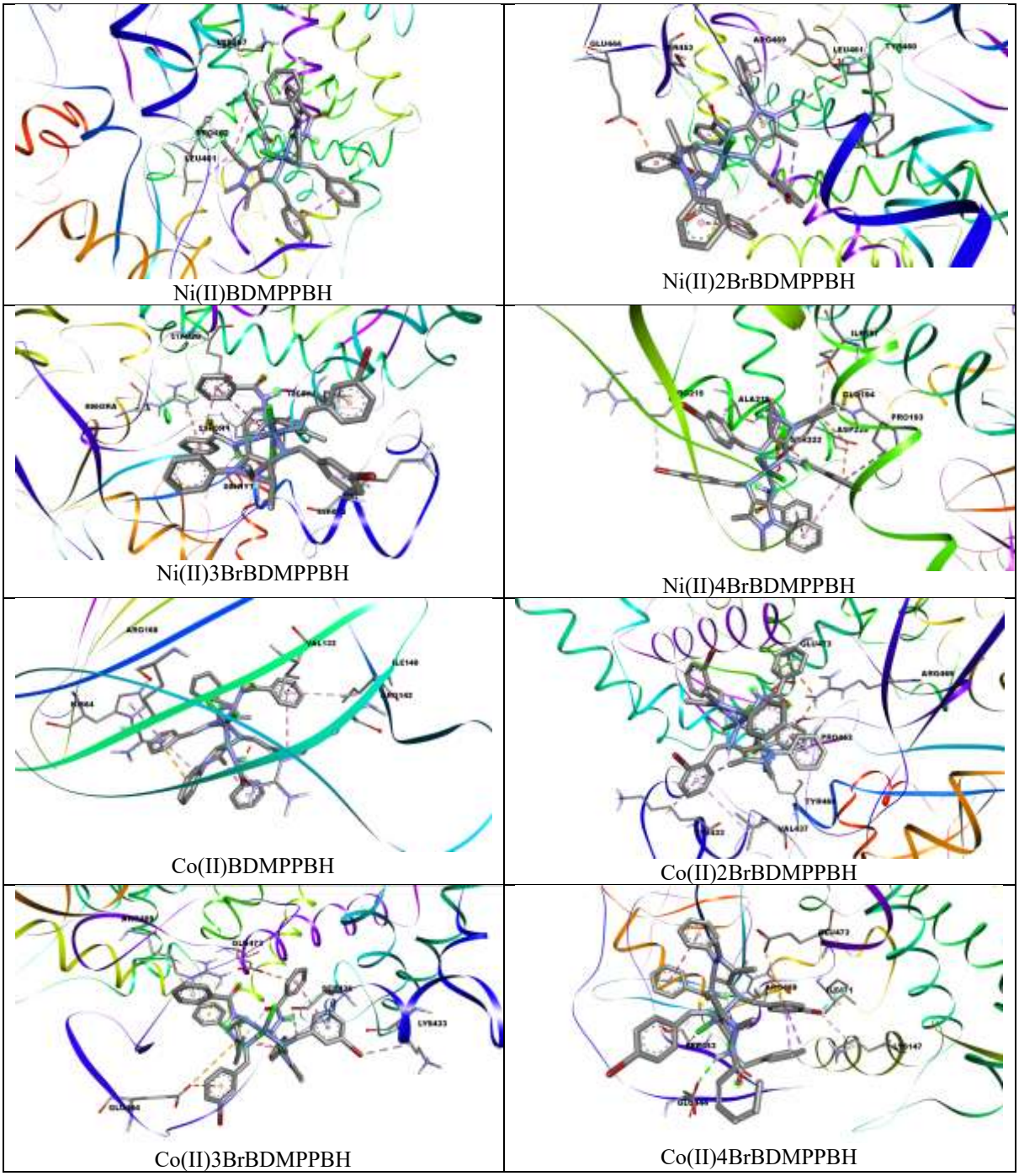

Figure 8: 3D Molecular docking study of Ni(II) and Co(II) complexes against Candida albicans lanosterol 14-α-demethylase

CONCLUSION

The Novel Ni(II) and Co(II) complexes of 4-aminoantipyrine derivatives were synthesized and characterised by various spectroscopic techniques. IR spectra shows coordination of azomethine nitrogen with central metal ion. The synthesized Novel Ni (II) and Co(II) complexes were thermally stable upto 300 ^{0}C. The Ni(II) and Co(II) complexes shows greater microbial activity against the tested microorganism compare to their respective parent derivatives which shows chelation increases the lipophilicity of metal complexes as per Tweedy's Chelation theory. Among all investigated novel complexes of Ni(II) and Co(II), Co(II)3BrBDMPPBH, Co(II)2BrBDMPPBH and Ni(II)4BrBDMPPBH emerged as the most promising antifungal candidates, whereas Ni(II)2BrBDMPPBH and Co(II)2BrBDMPPBH demonstrated the highest antibacterial potential against DNA gyrase B. The observed interaction patterns indicate that both electrostatic interactions (π-cation and π-anion) together with hydrophobic contacts and hydrogen bonding collectively contribute to stable binding and may underlie the predicted biological activities of these metal complexes.

Acknowledgement:

The author expresses their heartfelt gratitude to the Principal and Management of Kirti M. Doongursee College, Dadar for their constant support and motivation for this research work.

REFERENCES

(1) Joseph, J.; Nagashri, K.; Rani, G. A. B. Synthesis, Characterization and Antimicrobial Activities of Copper Complexes Derived from 4-Aminoantipyrine Derivatives. *Journal of Saudi Chemical Society* **2013**, *17* (3), 285–294. https://doi.org/10.1016/j.jscs.2011.04.007.

(2) Saini, M. S.; Kumar, A.; Dwivedi, J.; Singh, R. A REVIEW: BIOLOGICAL SIGNIFICANCES OF HETEROCYCLIC COMPOUNDS.

(3) Issa, R. M.; Khedr, A. M.; Rizk, H. F. UV–Vis, IR and 1H NMR Spectroscopic Studies of Some Schiff Bases Derivatives of 4-Aminoantipyrine. *Spectrochimica Acta Part A: Molecular and Biomolecular Spectroscopy* **2005**, *62* (1–3), 621–629. https://doi.org/10.1016/j.saa.2005.01.026.

(4) Obasi, L. N.; Kaior, G. U.; Rhyman, L.; Alswaidan, I. A.; Fun, H.-K.; Ramasami, P. Synthesis, Characterization, Antimicrobial Screening and Computational Studies of 4-[3-(4-Methoxy-Phenyl)-Allylideneamino]-1,5-Dimethyl-2-Phenyl-1,2-Dihydro-Pyrazol-3-One. *Journal of Molecular Structure* **2016**, *1120*, 180–186. https://doi.org/10.1016/j.molstruc.2016.05.037.

(5) Anupama, B.; Aruna, A.; Manga, V.; Sivan, S.; Sagar, M. V.; Chandrashekar, R. Synthesis, Spectral Characterization, DNA/ Protein Binding, DNA Cleavage, Cytotoxicity, Antioxidative and Molecular Docking Studies of Cu(II)Complexes Containing Schiff Base-Bpy/Phen Ligands. *J Fluoresc* **2017**, *27* (3), 953–965. https://doi.org/10.1007/s10895-017-2030-5.

(6) Alam, M. S.; Lee, D.-U. Synthesis, Molecular Structure and Antioxidant Activity of (E)-4-[Benzylideneamino]-1,5-Dimethyl-2-Phenyl-1H-Pyrazol-3(2H)-One, a Schiff Base Ligand of 4-Aminoantipyrine. *J Chem Crystallogr* **2012**, *42* (2), 93–102. https://doi.org/10.1007/s10870-011-0209-1.

(7) Shoaib, M.; Rahman, G.; Ali Shah, S. W.; Umar, M. N. Synthesis of 4-Aminoantipyrine Derived Schiff Bases and Their Evaluation for Antibacterial, Cytotoxic and Free Radical Scavenging Activity. *Bangladesh J Pharmacol* **2015**, *10* (2), 332. https://doi.org/10.3329/bjp.v10i2.22471.

(8) Ghorab, M.; El-Gazzar, M.; Alsaid, M. Synthesis, Characterization and Anti-Breast Cancer Activity of New 4-Aminoantipyrine-Based Heterocycles. *IJMS* **2014**, *15* (5), 7539–7553. https://doi.org/10.3390/ijms15057539.

(9) Abdulghani, A. J.; Ahmed, Z. Z. Synthesis, Structure and Characterization of New Metal Complexes of Schiff Bases Derived from Isatin N-Benzylisatin and 4-Aminoantipyrine. *Pak. J. Chem* **2011**, *1* (3), 100–113. https://doi.org/10.15228/2011.v01.i03.p01.

(10) Al-Gaber, M. A. I.; Abd El-Lateef, H. M.; Khalaf, M. M.; Shaaban, S.; Shawky, M.; Mohamed, G. G.; Abdou, A.; Gouda, M.; Abu-Dief, A. M. Design, Synthesis, Spectroscopic Inspection, DFT and Molecular Docking Study of Metal Chelates Incorporating Azo Dye Ligand for Biological Evaluation. *Materials* **2023**, *16* (3), 897. https://doi.org/10.3390/ma16030897.

(11) Baluja, S.; Chanda, S. Synthesis, Characterization and Antibacterial Screening of Some Schiff Bases Derived from Pyrazole and 4-Amino Antipyrine. *Rev. Colomb. Cienc. Quim. Farm.* **2016**, *45* (2), 201. https://doi.org/10.15446/rcciquifa.v45n2.59936.

(12) Manjula, B.; Antony, S. A.; Dhanaraj, C. J. Synthesis, Spectral Characterization, and Antimicrobial Activities of Schiff Base Complexes Derived From 4-Aminoantipyrine. *Spectroscopy Letters* **2014**, *47* (7), 518–526. https://doi.org/10.1080/00387010.2013.820196.

(13) Selwin Joseyphus, R.; Shiju, C.; Joseph, J.; Justin Dhanaraj, C.; Arish, D. Synthesis and Characterization of Metal Complexes of Schiff Base Ligand Derived from Imidazole-2-Carboxaldehyde and 4-Aminoantipyrine. *Spectrochimica Acta Part A: Molecular and Biomolecular Spectroscopy* **2014**, *133*, 149–155. https://doi.org/10.1016/j.saa.2014.05.050.

(14) Al Wagaa, F. Ali.; Ahmed, S. Ali. Nano-Schiff Base Ligand:Synthesis, Characterization, DFT, and Antibacterial Evaluation of Some Complexes Derived From 4-(-4-Methoxybenzylidene)Amino) -Antipyrinyl with Glycine Amino Acid Ligand. *J. Phys.: Conf. Ser.* **2021**, *1999* (1), 012003. https://doi.org/10.1088/1742-6596/1999/1/012003.

(15) Tyagi, M.; Chandra, S.; Tyagi, P.; Akhtar, J.; Kandan, A.; Singh, B. Synthesis, Characterization and Anti-Fungal Evaluation of Ni(II) and Cu(II) Complexes with a Derivative of 4-Aminoantipyrine. *Journal of Taibah University for Science* **2017**, *11* (1), 110–120. https://doi.org/10.1016/j.jtusci.2015.11.003.
(16) Kashyap, S.; Kumar, S.; Ramasamy, K.; Lim, S. M.; Shah, S. A. A.; Om, H.; Narasimhan, B. Synthesis, Biological Evaluation and Corrosion Inhibition Studies of Transition Metal Complexes of Schiff Base. *Chemistry Central Journal* **2018**, *12* (1), 117. https://doi.org/10.1186/s13065-018-0487-1.
(17) Ossai, V.; Obiefuna, A. P.; Laraps, B. C.; Okenyeka, O. U.; Ezeorah, J. C.; Dege, N.; Ibezim, A.; Lutter, M.; Jurkschat, K.; Obasi, N. L. Crystal Structural and in Silico Studies of Schiff Bases Derived from 4-Aminoantipyrine. *Solid State Sciences* **2020**, *106*, 106293.
https://doi.org/10.1016/j.solidstatesciences.2020.106293.
(18) Teran, R.; Guevara, R.; Mora, J.; Dobronski, L.; Barreiro-Costa, O.; Beske, T.; Pérez-Barrera, J.; Araya-Maturana, R.; Rojas-Silva, P.; Poveda, A.; Heredia-Moya, J. Characterization of Antimicrobial, Antioxidant, and Leishmanicidal Activities of Schiff Base Derivatives of 4-Aminoantipyrine. *Molecules* **2019**, *24* (15), 2696. https://doi.org/10.3390/molecules24152696.
(19) Erturk, A. G. Synthesis, Structural Identifications of Bioactive Two Novel Schiff Bases. *Journal of Molecular Structure* **2020**, *1202*, 127299. https://doi.org/10.1016/j.molstruc.2019.127299.
(20) Mjos, K. D.; Orvig, C. Metallodrugs in Medicinal Inorganic Chemistry. *Chem. Rev.* **2014**, *114* (8), 4540–4563. https://doi.org/10.1021/cr400460s.
(21) Ndagi, U.; Mhlongo, N.; Soliman, M. Metal Complexes in Cancer Therapy – an Update from Drug Design Perspective. *DDDT* **2017**, *Volume11*, 599–616. https://doi.org/10.2147/DDDT.S119488.
(22) Raman, N.; Thangaraja, C.; Johnsonraja, S. Synthesis, Spectral Characterization, Redox and Antimicrobial Activity of Schiff Base Transition Metal(II) Complexes Derived from 4-Aminoantipyrine and 3-Salicylideneacetylacetone. *Open Chemistry* **2005**, *3* (3), 537–555. https://doi.org/10.2478/BF02479281.
(23) Omar, M. M.; Mohamed, G. G.; Ibrahim, A. A. Spectroscopic Characterization of Metal Complexes of Novel Schiff Base. Synthesis, Thermal and Biological Activity Studies. *Spectrochimica Acta Part A: Molecular and Biomolecular Spectroscopy* **2009**, *73* (2), 358–369. https://doi.org/10.1016/j.saa.2009.02.043.
(24) Raman, N.; Raja, J. D.; Sakthivel, A. Design, Synthesis, Spectroscopic Characterization, Biological Screening, and DNA Nuclease Activity of Transition Metal Complexes Derived from a Tridentate Schiff Base. *Russ J Coord Chem* **2008**, *34* (6), 400–406. https://doi.org/10.1134/S107032840806002X.
(25) Chandra, S.; Jain, D.; Sharma, A. K.; Sharma, P. Coordination Modes of a Schiff Base Pentadentate Derivative of 4-Aminoantipyrine with Cobalt(II), Nickel(II) and Copper(II) Metal Ions: Synthesis, Spectroscopic and Antimicrobial Studies. *Molecules* **2009**, *14* (1), 174–190. https://doi.org/10.3390/molecules14010174.
(26) Raman, N.; Johnson Raja, S.; Sakthivel, A. Transition Metal Complexes with Schiff-Base Ligands: 4-Aminoantipyrine Based Derivatives–a Review. *Journal of Coordination Chemistry* **2009**, *62* (5), 691–709. https://doi.org/10.1080/00958970802326179.
(27) Sharma, A. K.; Chandra, S. Spectroscopic and Mycological Studies of Co(II), Ni(II) and Cu(II) Complexes with 4-Aminoantipyrine Derivative. *Spectrochimica Acta Part A: Molecular and Biomolecular Spectroscopy* **2011**, *81* (1), 424–430. https://doi.org/10.1016/j.saa.2011.06.032.
(28) Agarwal, R. K.; Prasad, S. Synthesis, Spectroscopic and PhysicochemicalCharacterization and Biological Activity of Co(II)and Ni(II) Coordination Compounds with 4-Aminoantipyrine Thiosemicarbazone. *Bioinorganic Chemistry and Applications* **2005**, *3* (3–4), 271–288. https://doi.org/10.1155/BCA.2005.271.
(29) Synthesis, Spectral Characterization and Antimicrobial Studies of Schiff Base Transition Metal Complexes Derived from Cuminaldehyde and 4-Aminoantipyrine. *Chem Sci Trans* **2014**.
https://doi.org/10.7598/cst2014.805.
(30) Raman, N.; Dhaveethu Raja, J.; Sakthivel, A. Synthesis, Spectral Characterization of Schiff Base Transition Metal Complexes: DNA Cleavage and Antimicrobial Activity Studies. *J Chem Sci* **2007**, *119* (4), 303–310. https://doi.org/10.1007/s12039-007-0041-5.
(31) Leovac, V. M.; Novaković, S. B.; Bogdanović, G. A.; Joksović, M. D.; Mészáros Szécsényi, K.; Češljević, V. I. Transition Metal Complexes with Thiosemicarbazide-Based Ligands. Part LVI: Nickel(II) Complex with 1,3-Diphenylpyrazole-4-Carboxaldehyde Thiosemicarbazone and Unusually Deformed Coordination Geometry. *Polyhedron* **2007**, *26* (14), 3783–3792. https://doi.org/10.1016/j.poly.2007.04.012.
(32) Selwin Joseyphus, R.; Shiju, C.; Joseph, J.; Justin Dhanaraj, C.; Arish, D. Synthesis and Characterization of Metal Complexes of Schiff Base Ligand Derived from Imidazole-2-Carboxaldehyde and 4-Aminoantipyrine. *Spectrochimica Acta Part A: Molecular and Biomolecular Spectroscopy* **2014**, *133*, 149–155.
https://doi.org/10.1016/j.saa.2014.05.050.
(33) Mestry, K. A.; Meher, C. B.; Khan, S. M.; Patil, D. V.; Jadhav, V. D.; Yedage, D. B.; Vhatkar, M. V.; Palande, S. V. Eco-Friendly Synthesis Of 4-Aminoantipyrine Derivatives And Biological Potential Evaluation Of Some Novel Derivatives With Their Computational Study. **2026**, *13* (2).
(34) Selwin Joseyphus, R.; Shiju, C.; Joseph, J.; Justin Dhanaraj, C.; Arish, D. Synthesis and Characterization of Metal Complexes of Schiff Base Ligand Derived from Imidazole-2-Carboxaldehyde and 4-Aminoantipyrine. *Spectrochimica Acta Part A: Molecular and Biomolecular Spectroscopy* **2014**, *133*, 149–155.
https://doi.org/10.1016/j.saa.2014.05.050.

(35) Selwin Joseyphus, R.; Shiju, C.; Joseph, J.; Justin Dhanaraj, C.; Arish, D. Synthesis and Characterization of Metal Complexes of Schiff Base Ligand Derived from Imidazole-2-Carboxaldehyde and 4-Aminoantipyrine. *Spectrochimica Acta Part A: Molecular and Biomolecular Spectroscopy* **2014**, *133*, 149–155. https://doi.org/10.1016/j.saa.2014.05.050.
(36) Abdulghani, A. J.; Ahmed, Z. Z. Synthesis, Structure and Characterization of New Metal Complexes of Schiff Bases Derived from Isatin N-Benzylisatin and 4-Aminoantipyrine. *Pak. J. Chem* **2011**, *1* (3), 100–113. https://doi.org/10.15228/2011.v01.i03.p01.
(37) Joseph, J.; Nagashri, K.; Rani, G. A. B. Synthesis, Characterization and Antimicrobial Activities of Copper Complexes Derived from 4-Aminoantipyrine Derivatives. *Journal of Saudi Chemical Society* **2013**, *17* (3), 285–294. https://doi.org/10.1016/j.jscs.2011.04.007.